

## Ferromagnetism of Co-doped TiO<sub>2</sub>(B) nanotubes

X. W. Wang, X. P. Gao,<sup>a)</sup> G. R. Li, L. Gao, and T. Y. Yan  
*Institute of New Energy Material Chemistry, Nankai University, Tianjin 300071, China*

H. Y. Zhu<sup>b)</sup>  
*School of Physical and Chemical Sciences, Queensland University of Technology, Brisbane QLD 4001, Australia*

(Received 25 June 2007; accepted 5 September 2007; published online 1 October 2007)

The Co-doped titanate nanotubes, synthesized via a hydrothermal reaction, are calcined at 300, 400, and 500 °C for 2 h in an argon atmosphere to yield Co-doped TiO<sub>2</sub>(B) nanotubes and anatase nanotubes with a dark gray color. It is shown that all calcined titania nanotubes have a stronger absorption in visible region, attributed to the formation of oxygen vacancies. The saturation magnetization of all Co-doped titania nanotubes is stronger than that of as-prepared Co-doped titanate nanotubes. In particular, Co-doped TiO<sub>2</sub>(B) nanotubes calcined at 300 °C exhibit the strongest ferromagnetism due to the existence of oxygen vacancies, as confirmed further by electron paramagnetic resonance spectra. © 2007 American Institute of Physics. [DOI: 10.1063/1.2789734]

The titanium oxides with one-dimensional (1D) nanostructures, such as nanotubes, nanorods, and nanowires, are of particular significance because their unique morphology and microstructure bring several important features. The titania nanotubes have been found to be very attractive due to their superior physicochemical properties as active materials for photocatalysis,<sup>1,2</sup> photoelectrochemistry,<sup>3-5</sup> lithium storage.<sup>6-11</sup> Following the discovery by Matsumoto *et al.* in 2001 of room temperature ferromagnetism in Co-doped TiO<sub>2</sub> anatase film,<sup>12</sup> more attentions have been focused on Co-doped TiO<sub>2</sub> film, nanocrystals, and nanorods.<sup>13,14</sup> Recently, Co/Fe-doped titanate nanotubes and Co-doped anatase nanotubes with room temperature ferromagnetism have been reported for potential applications in spintronics.<sup>15-19</sup> It is believed that the appearance of oxygen vacancies near Co<sup>2+</sup> sites in Co-doped TiO<sub>2</sub> has important influence on the room temperature ferromagnetism.<sup>18</sup>

Among titania polymorphs [including anatase, rutile, TiO<sub>2</sub>(B), and brookite], monoclinic TiO<sub>2</sub>(B) as a *n*-type semiconductor has a relatively open tunnel structure and a low density as compared with other titania polymorphs. TiO<sub>2</sub>(B) nanotubes have shown excellent electrochemical lithium storage and photocatalytic dehydrogenation of ethanol.<sup>20-23</sup> Abundant surface states or oxygen vacancies were reported to exist in TiO<sub>2</sub>(B) with 1D nanostructure.<sup>24</sup> Co-doped TiO<sub>2</sub>(B) nanotubes would have an improved ferromagnetism due to the metastable phase and more structure defects.

In this work, Co-doped titanate nanotubes were prepared through a hydrothermal reaction and converted into Co-doped TiO<sub>2</sub>(B) nanotubes after the calcination. An appropriate amount of cobalt nitrate Co(NO<sub>3</sub>)<sub>2</sub>·6H<sub>2</sub>O (8 at. %) was fully dissolved in a small amount of water (7 ml), and TiO<sub>2</sub> (anatase) powders were added in the solution and dispersed ultrasonically for 1 h. After that 11 M NaOH aqueous solution (43 ml) was transferred to the solution and mixed sufficiently under an ultrasonic treatment. The hydrothermal reaction was conducted at 130 °C for 48 h in a Teflon autoclave (50 ml/65 ml). The products were thoroughly

washed with distilled water and 0.1 M HCl to a pH value of about 7 and dried at 100 °C. A ceramic boat with the as-prepared sample was located in the center of a tubular furnace. Then argon gas was introduced to the above furnace at a flow rate of 100 SCCM (SCCM denotes cubic centimeters per minute at STP) for 1 h prior to the calcination. The as-prepared sample was heated to 300, 400, and 500 °C at a rate of 10 °C/min and kept for 2 h in argon atmosphere. The microstructure of the samples was characterized using x-ray diffraction (XRD) (Rigaku D/max-2500), and transmission electron microscopy (TEM) (FEI Tecnai 20). Elemental analysis of cobalt was conducted on a Thermo Jarrell-Ash model inductively coupled plasma emission spectrometer (ICPES) [9000(N+M)]. N<sub>2</sub> adsorption data were measured using NOVA 2000e (Quantachrome) instrument and the specific surface area was calculated by the Brnauer-Emmett-Teller (BET) equation. The optical property was investigated by UV-visible spectrophotometer (Varian Cary-100). The magnetic property was measured using a superconducting interference device (MPMS-XL7, Quantum Design) at 300 K. Electron paramagnetic resonance (EPR) spectra were measured on a Bruker EMX-6/1 EPR spectrometer at room temperature.

XRD patterns of as prepared and calcined samples are given in Fig. 1. All diffraction peaks of the as-prepared sample can be assigned to layered protonated titanate (Ref. 25) with poor crystallinity.<sup>8,26</sup> It is also shown that the interlayer distance of nanotubes is reduced gradually with further increasing calcination temperature. After the calcination at 500 °C, the anatase phase seems to coexist with the metastable monoclinic TiO<sub>2</sub>(B) (Ref. 27), which is usually formed during the dehydration of layered titanate nanotubes at low temperature. When the as-prepared sample was calcined at 300 °C, only TiO<sub>2</sub>(B) phase with a poor crystallinity is obtained, in good agreement with the previous results.<sup>22,23,28</sup> In particular, the anatase phase is hardly formed after calcination at 400 °C in argon atmosphere, which usually coexists with TiO<sub>2</sub>(B) after calcination in air.<sup>22,29</sup> Therefore, the argon atmosphere used during calcination is important to prohibit the phase transition from TiO<sub>2</sub>(B) to anatase. However, no diffraction peaks of cobalt species can be detected in the XRD patterns.

<sup>a)</sup>Electronic mail: xpgao@nankai.edu.cn

<sup>b)</sup>Electronic mail: hy.zhu@qut.edu.au

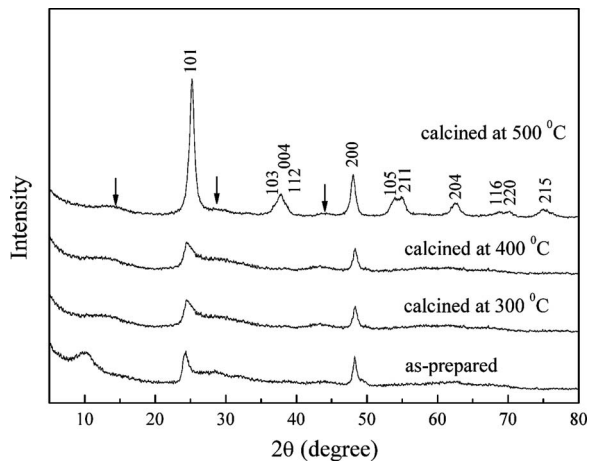


FIG. 1. XRD patterns of the as-prepared titanate nanotubes and calcined products at different temperatures.

The as-prepared Co-doped titanate nanotubes have an outer diameter of 10–15 nm [Fig. 2(a)] and BET specific surface area of 330 m<sup>2</sup>/g. The energy dispersive x-ray spectrum (EDS) [Fig. 2(e)] confirms the presence of cobalt element in the as-prepared Co-doped titanate nanotubes. The cobalt concentration is 0.9 at. % based from ICP analysis, much lower than the added amount before the hydrothermal reaction due to loss in the washing process. It means that a small amount of cobalt is doped in as-prepared nanotubes. After the calcination at 300 °C in argon atmosphere, the resultant TiO<sub>2</sub>(B) retains the same morphology with a smooth surface and a large specific surface area of 251 m<sup>2</sup>/g. When the as-prepared sample is calcined at 400 °C, TiO<sub>2</sub>(B) still remains the tubular morphology with some nanoparticles attached on the surface of nanotubes. After further increasing the calcination temperature to 500 °C, some nanotubes with the anatase structure are curved or collapse to some extent as compared with the as-prepared titanate nanotubes, resulting in a great decrease of the specific surface area (97 m<sup>2</sup>/g). Meanwhile, the wall of anatase nanotubes with a good crystallinity calcined at 500 °C becomes thicker as shown from high-resolution TEM image [inset in Fig. 2(d)]. In addition, rodlike morphology can be still observed among anatase nanotubes. The calcination in argon atmosphere is more favorable to avoid forming anatase phase with a solid nanorod morphology. Therefore, 300 °C is the optimal calcination temperature to achieve the TiO<sub>2</sub>(B) phase, which maintains the hollow tubular morphology with a clear surface.

It is noted that all Co-doped nanotubes calcined in argon atmosphere have a dark gray color, which show a stronger absorption in visible region as compared with the as-prepared Co-doped titanate nanotubes. While the absorption of the white Co-doped titania nanotubes calcined in air is usually negligible in visible region, similar to that of the as-prepared nanotubes.<sup>22,23</sup> It was reported that annealing of TiO<sub>2</sub> nanotubes in argon atmosphere increased the concentration of oxygen vacancies as defect density.<sup>30</sup> The strong absorption of the calcined Co-doped titania nanotubes in visible region is largely related to the formation of oxygen vacancies in the absence of O<sub>2</sub>.

It is found from Fig. 4 that the as-prepared Co-doped titanate nanotubes exhibit an evident hysteresis loops at 300 K, indicating ferromagnetic properties although the cobalt concentration in nanotubes is low. The saturation mag-

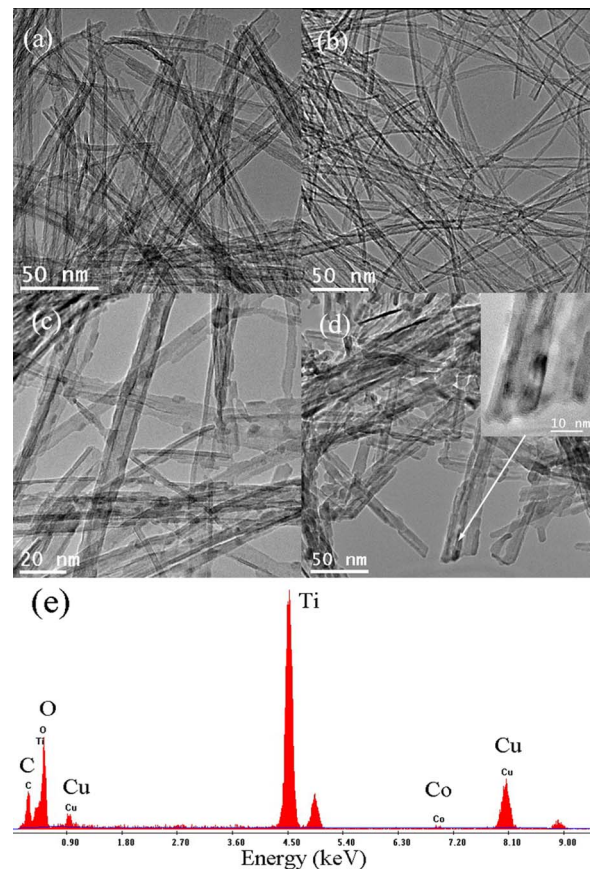


FIG. 2. (Color online) (a) TEM images of the as-prepared titanate nanotubes and calcined products at (b) 300, (c) 400, and (d) 500 °C. EDS spectrum of as-prepared titanate nanotubes is shown in (e).

netization ( $M_s$ ) of the as-prepared Co-doped titanate nanotubes is 0.000 723 emu/g. It was reported previously that oxygen vacancies near Co<sup>2+</sup> sites in Co-doped TiO<sub>2</sub> had an important contribution to the ferromagnetism.<sup>18,31–33</sup> Coey *et al.* proposed that oxygen vacancies induced the ferromagnetic coupling through a *F*-center exchange mechanism.<sup>33</sup> The saturation magnetization of all Co-doped titania nanotubes, calcined in argon atmosphere, is stronger than that of the as-prepared nanotubes due to the formation of extra oxygen vacancies during the calcination in the absence of O<sub>2</sub>. In the meantime, it is also demonstrated that the calcination temperature has a great influence on the saturation

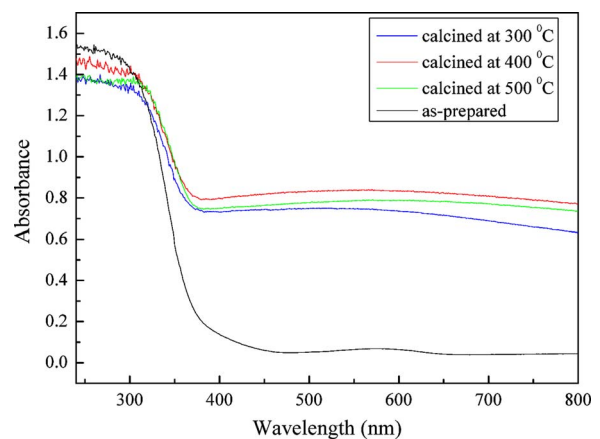


FIG. 3. (Color online) UV-visible diffuse-reflectance spectra of the Co-doped as-prepared titanate nanotubes and calcined products at different temperatures.

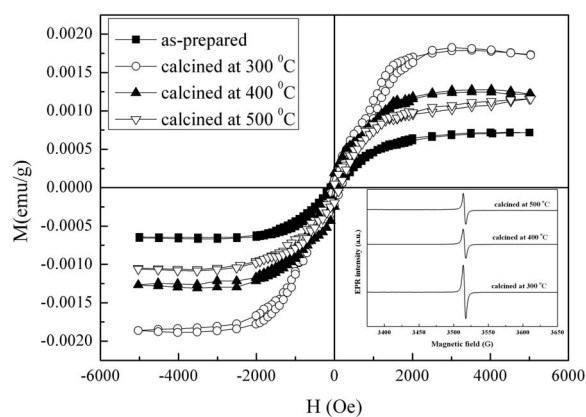


FIG. 4. Hysteresis loops at 300 K for the Co-doped as-prepared titanate nanotubes and calcined products at different temperatures. EPR spectra of Co-doped nanotubes calcined at different temperatures are inserted.

magnetization of Co-doped nanotubes. In particular, Co-doped  $\text{TiO}_2(\text{B})$  nanotubes with a poor crystallinity calcined at 300 °C have the strongest ferromagnetism. With further increasing calcination temperature to 500 °C, the saturation magnetization of Co-doped nanotubes turns to decrease. As shown by XRD patterns, the calcination at 500 °C results in  $\text{TiO}_2(\text{B})$  partially transforming into anatase.  $\text{TiO}_2(\text{B})$  and anatase are structurally related, containing chains of edge-sharing octahedral in one orientation. The transformation from  $\text{TiO}_2(\text{B})$  to anatase occurs always with the shear eliminating a similar amount of cationic and anionic vacancies.<sup>34</sup> Therefore, the formation of anatase phase in the sample calcined at 500 °C results in decrease of oxygen vacancies, and further results in decrease of the saturation magnetization of Co-doped anatase nanotubes.

To further confirm the existence of oxygen vacancies, EPR spectra of the Co-doped titania nanotubes as inserted in Fig. 4. It is shown that all samples have the sharp symmetric EPR peak. The EPR signal with  $g=2.00$  was reported and referred to as a single-electron trapped oxygen vacancy of  $\text{TiO}_2$ .<sup>35</sup> The EPR signal relative intensity of Co-doped  $\text{TiO}_2(\text{B})$  nanotubes calcined at 300 °C is obviously higher than that of the samples calcined at the higher temperatures. The asymmetric EPR signal with  $g=1.97-1.98$  is not observed, which is usually originated from surface defects.<sup>35</sup> It implies that bulk oxygen vacancies rather than surface defects have more responsibility for the appearance of EPR signals in Co-doped  $\text{TiO}_2(\text{B})$  nanotubes. As shown above, the calcination at higher temperature results always in the formation of anatase phase with good crystallinity and less bulk defects. Therefore, more oxygen vacancies appear in Co-doped  $\text{TiO}_2(\text{B})$  nanotubes calcined at 300 °C, contributing to the strong ferromagnetism as measured above.

In summary, Co-doped titanate nanotubes can be synthesized via the hydrothermal reaction in concentrated alkaline solution, and converted to Co-doped  $\text{TiO}_2(\text{B})$  and anatase nanotubes by the calcination at different temperatures. The presence of cobalt element in the as-prepared titanate nanotubes is confirmed by EDS spectrum and the cobalt concentration is 0.9 at. % based from ICP analysis. All calcined Co-doped titania nanotubes, with a dark gray color, have a stronger absorption in visible region, attributed to the formation of oxygen vacancies in argon atmosphere. The saturation magnetization of all Co-doped titania nanotubes is stronger than that of the Co-doped titanate nanotubes due to the

formation of oxygen vacancies. In particular, Co-doped  $\text{TiO}_2(\text{B})$  nanotubes calcined at 300 °C have the strongest ferromagnetism due to the existence of oxygen vacancies, as confirmed further by EPR spectra.

This work is supported by the NCET (040219) and TNSF (07JCZDJC00400) of China. Financial supports from the ARC are also gratefully acknowledged.

- <sup>1</sup>X. Quan, S. G. Yang, X. L. Ruan, and H. M. Zhao, *Environ. Sci. Technol.* **39**, 3770 (2005).
- <sup>2</sup>H. Y. Zhu, Y. Lan, X. P. Gao, S. P. Ringer, Z. F. Zheng, D. Y. Song, and J. C. Zhao, *J. Am. Chem. Soc.* **127**, 6730 (2005).
- <sup>3</sup>G. K. Mor, K. Shankar, O. K. Varghese, and C. A. Grimes, *J. Mater. Res.* **19**, 2989 (2004).
- <sup>4</sup>Y. B. Xie, *Adv. Funct. Mater.* **16**, 1823 (2006).
- <sup>5</sup>A. Ghicov, B. Schmidt, J. Kunze, and P. Schmuki, *Chem. Phys. Lett.* **433**, 323 (2007).
- <sup>6</sup>Y. K. Zhou, L. Cao, F. B. Zhang, B. L. He, and H. L. Li, *J. Electrochem. Soc.* **150**, A1246 (2003).
- <sup>7</sup>X. P. Gao, Y. Lan, H. Y. Zhu, J. W. Liu, Y. P. Ge, F. Wu, and D. Y. Song, *Electrochem. Solid-State Lett.* **8**, A26 (2005).
- <sup>8</sup>J. R. Li, Z. L. Tang, and Z. T. Zhang, *Electrochem. Solid-State Lett.* **8**, A316 (2005).
- <sup>9</sup>Y. Lan, X. P. Gao, H. Y. Zhu, Z. F. Zheng, F. Wu, S. P. Ringer, and D. Y. Song, *Adv. Funct. Mater.* **15**, 1310 (2005).
- <sup>10</sup>J. Kim and J. Cho, *J. Electrochem. Soc.* **154**, A542 (2007).
- <sup>11</sup>Z. W. Zhao, Z. P. Guo, D. Wexler, Z. F. Ma, X. Wu, and H. K. Liu, *Electrochem. Commun.* **9**, 697 (2007).
- <sup>12</sup>Y. Matsumoto, M. Murakami, T. Shono, T. Hasegawa, T. Fukumura, M. Kawasaki, P. Ahmet, T. Chikyow, S. Koshihara, and H. Koinuma, *Science* **291**, 854 (2001).
- <sup>13</sup>S. A. Chambers, T. Droubay, C. M. Wang, A. S. Lea, R. F. C. Farrow, L. Folks, V. Deline, and S. Anders, *Appl. Phys. Lett.* **82**, 1257 (2003).
- <sup>14</sup>J. D. Bryan, S. A. Santangelo, S. C. Keveren, and D. R. Gamelin, *J. Am. Chem. Soc.* **127**, 15568 (2005).
- <sup>15</sup>X. M. Sun and Y. D. Li, *Chem.-Eur. J.* **9**, 2229 (2003).
- <sup>16</sup>D. Wu, Y. F. Chen, J. Liu, X. N. Zhao, A. D. Li, and N. B. Ming, *Appl. Phys. Lett.* **87**, 112501 (2005).
- <sup>17</sup>X. G. Xu, X. Ding, Q. Chen, and L. M. Peng, *Phys. Rev. B* **73**, 165403 (2006).
- <sup>18</sup>C. M. Huang, X. Q. Liu, Y. P. Liu, and Y. Y. Wang, *Chem. Phys. Lett.* **432**, 468 (2006).
- <sup>19</sup>C. Huang, X. Liu, L. Kong, W. Lan, Q. Su, and Y. Wang, *Appl. Phys. A: Mater. Sci. Process.* **87**, 781 (2007).
- <sup>20</sup>G. Armstrong, A. R. Armstrong, J. Canales, and P. G. Bruce, *Chem. Commun. (Cambridge)* **2005**, 2454.
- <sup>21</sup>G. Armstrong, A. R. Armstrong, J. Canales, and P. G. Bruce, *Electrochem. Solid-State Lett.* **9**, A139 (2006).
- <sup>22</sup>H. Zhang, G. R. Li, L. P. An, T. Y. Yan, X. P. Gao, and H. Y. Zhu, *J. Phys. Chem. C* **111**, 6143 (2007).
- <sup>23</sup>H. L. Kuo, C. Y. Kuo, C. H. Liu, J. H. Chao, and C. H. Lin, *Catal. Lett.* **113**, 7 (2007).
- <sup>24</sup>G. Wang, Q. Wang, W. Lu, and J. H. Li, *J. Phys. Chem. B* **110**, 22029 (2006).
- <sup>25</sup>JCPDS Card No. 47-0124.
- <sup>26</sup>Q. Chen, W. Z. Zhou, G. H. Du, and L. M. Peng, *Adv. Mater. (Weinheim, Ger.)* **14**, 1208 (2002).
- <sup>27</sup>JCPDS Card No. 35-0088.
- <sup>28</sup>M. Qamar, C. R. Yoon, H. J. Oh, D. H. Kim, J. H. Jho, K. S. Lee, W. J. Lee, H. G. Lee, and S. J. Kim, *Nanotechnology* **17**, 5922 (2006).
- <sup>29</sup>L. Z. Zhang, H. Lin, N. Wang, C. F. Lin, and J. B. Li, *J. Alloys Compd.* **431**, 230 (2007).
- <sup>30</sup>P. Pillai, K. S. Raja, and M. Misra, *J. Power Sources* **161**, 524 (2006).
- <sup>31</sup>Y. X. Wang, H. Liu, Z. Q. Li, X. X. Zhang, R. K. Zheng, and S. P. Ringer, *Appl. Phys. Lett.* **89**, 042511 (2006).
- <sup>32</sup>L. G. Kong, J. F. Kang, Y. Wang, L. Sun, L. F. Liu, X. Y. Liu, X. Zhang, and R. Q. Han, *Electrochem. Solid-State Lett.* **9**, G1 (2006).
- <sup>33</sup>J. M. D. Coey, A. P. Douvalis, C. B. Fitzgerald, and M. Venkatesan, *Appl. Phys. Lett.* **84**, 1332 (2004).
- <sup>34</sup>W. A. Daoud and G. K. H. Pang, *J. Phys. Chem. B* **110**, 25746 (2006).
- <sup>35</sup>J. M. Cho, W. J. Yun, J. K. Lee, H. S. Lee, W. W. So, S. J. Moon, Y. Jia, H. Kulkarni, and Y. Wu, *Appl. Phys. A: Mater. Sci. Process.* **88**, 751 (2007).